Modelling of ductile crack growth in welded joints using micromechanical failure criterion

M. Rakin[1,a], N. Gubeljak[2], M. Dobrojević[3], B. Međo[1], A. Sedmak[4]

[1] Faculty of Technology and Metallurgy, University of Belgrade, Karnegijeva 4, 11000 Belgrade, Serbia

[2] Faculty of Mechanical Engineering, University of Maribor, Smetanova 17, SI2000 Maribor, Slovenia

[3] Innovative Centre of Faculty of Mechanical Engineering, Kraljice Marije 16, 11000 Belgrade, Serbia

[4] Faculty of Mechanical Engineering, University of Belgrade, Kraljice Marije 16, 11000 Belgrade, Serbia

[a] marko@tmf.bg.ac.yu

Keywords: Micromechanical analysis, ductile fracture, crack initiation, crack growth, welded joints, finite element method.

Abstract. In this paper, ductile crack growth in strength mismatched welded joints is considered. High-strength low-alloyed (HSLA) steel in quenched and tempered condition is used as the base metal. Two different fillers are selected to obtain over- and undermatched weld metal. The flux-cored arc-welding process in shielding gas is applied. Constraint effect is tested by varying widths of the welded joints – three different weld metal widths are used: 6, 12 and 18 mm. Single-edged notched bend specimens (SENB) are experimentally and numerically analysed. Fatigue pre-crack is located in weld metal for all tested specimens (a_0/W = 0.32). Ductile crack growth initiation and stable crack growth are modelled using the coupled micromechanical model proposed by Gurson, Tvergaard and Needleman (GTN model). A comparison of force F vs. crack tip opening displacement (CTOD) curves during crack growth is given as determined both experimentally and numerically using the GTN model for the later. Failure criterion used in numerical analysis is discussed in detail.

Introduction

Properties of welded joints have a strong influence on the behaviour of welded constructions and structures. In analysis of a welded joint, at least three different materials should be considered: weld metal (WM), base metal (BM) and heat affected zone (HAZ). However, if the crack is located in the weld metal and runs along the material centre line, and the size of the heat affected zone is small – the effect of this zone can be neglected. These conditions are fulfilled for the problem analysed in this paper, and two-material idealisation of the welded joint is considered. The effect of the heterogeneity is quantified as the yield strength ratio of the materials making the joint – mismatch ratio. Depending on its value, joint can be over- or undermatched [1]. However, the mismatch ratio is not the only factor that influences the analysis, and the width of the welded joint should also be taken into account. The welded joint width affects the stress and strain distribution near the crack tip, which in turn affects the change of constraint in the weld metal [2,3].

Standard parameters of fracture mechanics, like stress-intensity factor, crack opening displacement and J-integral, cannot reliably describe the reaction of the pre-cracked material to external loading in all conditions. Even if these parameters could be applied and calculated for the tested specimen, the question is how to apply the results in the analysis of a real structure, having in mind dependence of these parameters on shape and size of the specimen. The micromechanical or

local approach to fracture seems appropriate for modelling these cases, as it correlates the local stresses and strains with fracture toughness [4,5].

The analysis of the crack growth is essential for welded joints integrity assessment, especially for high-strength steels. Parameters which may depend on external load, size and shape of the specimen or part of the real structure, are obtained using micromechanical analysis and modelling of fracture. Criteria of crack initiation and crack growth in welded joint are defined using micromechanical model of Gurson, Tvergaard and Needleman (GTN model). Crack growth simulation is performed using these critical values together with node release method. It is proved that combined technique of the local approach and node release method is capable of obtaining reliable results, even in the analysed case of heterogeneous materials, i.e. welded joints.

Micromechanical model

GTN model is based on the hypothesis that void nucleation and growth in metal can be macroscopically described by extending the von Mises plasticity theory to cover the effects of porosity occurring in the material. The void volume fraction, f, is introduced as a variable into the expression for plastic potential [6,7]:

$$\phi = \frac{3\sigma_{ij}^{'}\sigma_{ij}^{'}}{2\sigma^2} + 2q_1 f^* \cosh\left(\frac{3q_2\sigma_m}{2\sigma}\right) - \left[1 + (q_1 f^*)^2\right] = 0 \tag{1}$$

where σ denotes the actual yield stress of the material matrix, $\sigma_{ij}^{'}$ is the stress deviator, the parameters q_1 and q_2 were introduced by Tvergaard and Needleman [7] to improve the ductile fracture prediction of the Gurson model [6] and f^* is a function of the void volume fraction:

$$f^* = \begin{cases} f & for\, f \le f_c \\ f_c + K(f - f_c) & for\, f > f_c \end{cases} \tag{2}$$

where f_c is the critical value at which void coalescence occurs. The parameter K defines the slope of a sudden drop of the force on the force - diameter reduction diagram, and is often referred to as "accelerating factor". This factor defines the final stage of ductile fracture following the mechanism of void coalescence, which leads to complete loss of the load carrying capacity of the material:

$$K = \frac{f_U^* - f_c}{f_F - f_c}, \tag{3}$$

where the parameter f_U^* is related to q_1 by $f_U^* = 1/q_1$, while the void volume fraction at final fracture is designated by f_F. Once one of the conditions $f^* = f_U^*$ or $f = f_F$ is met, the considered material point loses its stiffness.

Initial void volume fraction, f_0, depends on the volume fraction of non-metallic inclusions in steel, f_V. Under plastic strain, voids in the metal matrix first nucleate around these inclusions, and in the final stage of ductile fracture, the voids may intensively nucleate around the secondary-phase particles.

Materials

The base metal (BM) is high-strength low-alloyed (HSLA) steel NIOMOL 490, which is often used for steel constructions. The flux-cored arc-welding (FCAW) process in shielding gas is applied and two different fillers are chosen: FITUB 75 and VAC 60 (designation according to producer

"Elektrode Jesenice"). The first one ensures overmatching (OM) and the second is used for obtaining undermatched (UM) welds. Details about welding process and preparation of the plates for X-grooved multipass welded joints are given in [3], while chemical compositions of the materials can be found in [8]. Basic mechanical properties of the materials, determined on round tensile (RT) specimens, are given in Table 1. The true stress – true strain diagrams of the materials can be found in [8].

Table 1: Mechanical properties of the materials

	OM	BM	UM
E [GPa]	183.8	202.9	206.7
$R_{p0.2}$ [MPa]	648	545	469
R_m [MPa]	744	648	590
M [$R_{p0.2\ WM}/R_{p0.2\ BM}$]	1.19	–	0.86

Microstructural observation of the materials reveals the presence of sulphides, oxides, silicates and complex inclusions. The highest fraction of sulphides and silicates is found in the UM weld metal, while in BM and OM a significant fraction of oxides exists (for details, see [9]). A micrograph with clusters of oxides in BM is shown in Fig. 1.

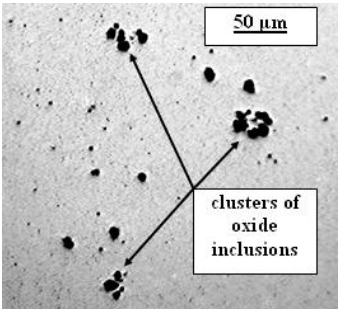

Fig. 1: Optical micrograph of non-metallic inclusions in BM

Initial void volume fraction, f_0, is determined by quantitative optical microscopy. Volume fraction of sulphides and oxides in tested steel, V_V, is determined based on equality with surface fraction, A_A [10]. Volume fraction f_V (see Table 2) is determined as the mean value of volume fraction of non-metallic inclusions for all measurement fields. Microstructural observations on low-alloyed steel with 0.22 wt% of carbon given in [11] shown that the effect of secondary voids formed around Fe_3C particles is extremely low and present only during the final stage of ductile fracture. Considering that the percentage of carbon in the base metal and fillers (0.04–0.123 wt%, see [8]) is lower in comparison with the investigation from [11], the fraction of Fe_3C is small and initiation of the secondary-voids is neglected in this paper. Therefore, it is assumed that the initial void volume fraction, f_0, is equal to the volume fraction f_V, according to [11,10].

In order to determine mean free path between non-metallic inclusions according to [10], in each measurement field five horizontal measuring (scan) lines are drawn. Then the value of N_L is determined, representing the number of interception of oxides or sulphides per measurement line unit (in mm). The mean free path, λ, is determined as the mean edge-to-edge distance between inclusions. The average value of mean free path λ is determined based on calculated values of λ in all measurement fields.

Table 2: Parameters of microstructure

Material (HSLA steel)	f_V	λ [μm]
BM	0.012164	103.1336
UM	0.007057	126.2614
OM	0.006342	157.4719

Experimental and numerical analysis

The SENB specimens are used for estimation of fracture behaviour of welded joints with various widths. The specimens were fatigue precracked in accordance with [12]. Fatigue precrack length is the same (a_0/W = 0.32) for all specimens. Single specimen method is used and DC potential drop technique is applied for stable crack monitoring. CTOD values are directly measured using d_5 clip gauge, developed by GKSS [13]. Welded joints are considered as bimetals consisting of base metal (BM) and weld metal (WM), (Fig. 2). The loading of both specimens is controlled by prescribed displacements. Three different widths of weld metal for both OM and UM welded joints are used: $2H$ = 6,12 and 18 mm.

Numerical analysis is conducted using Finite Element software ABAQUS (www.simulia.com), with GTN model integrated into the software. Round tensile specimen is considered as axisymmetrical, while SENB specimen is analysed under plane strain conditions. Isoparametric quadrilateral eight-node finite elements with reduced (2 x 2) Gauss integration are used. Fig. 2 shows finite element mesh of the SENB specimen. Due to the symmetry, one half of the specimen is modelled. The supporting cylinder and the cylinder where the load is applied are modelled as rigid bodies.

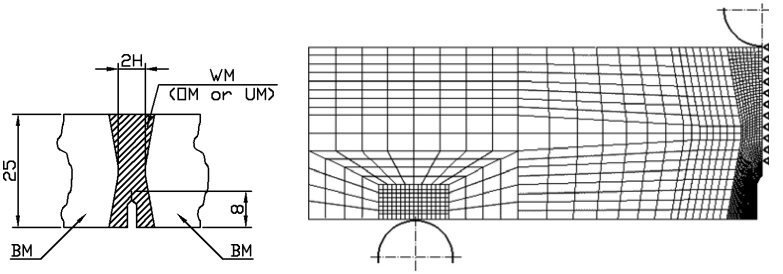

Fig. 2: FE mesh of SENB specimen and boundary conditions

The initial values of void volume fraction, f_0, for all three materials are adopted according to microstructural observations given in Table 2. Computations are conducted with values q_1 = 1.5 and q_2 = 1, which are commonly used values for these parameters, see [12,14]. Quadrilateral finite elements 0.15 x 0.15 mm are used in the vicinity of the crack tip. This element size is chosen according to the recommendations in [14] and [15], since it approximates the value of the mean free path between non-metallic inclusions in tested materials. More details about the influence of the element size on ductile fracture can be found in [8,14].

Critical void volume fraction, f_c, is determined by elastic–plastic FE analysis of the round tensile (RT) specimen. The values of f_c for all materials (BM, UM and OM) are determined using a combined experimental–numerical method; details can be found in [15,16]. The values of f_c determined on RT specimens are used for prediction of crack growth initiation on SENB specimens. According to [14], the condition corresponding to the crack growth initiation on a precracked geometry is defined by the instant when the first element in front of the crack tip becomes damaged. However, other definitions are discussed in [14,17]. In [15], it is shown that the condition for the

onset of crack growth as determined by the J-integral at initiation, J_i, is most adequately defined by the micromechanical criterion $f \geq f_c$ for the Gauss point nearest to the crack tip, where the value of f is highest. Thus, during numerical calculation, the increase of the void volume fraction f should be monitored at that Gauss point.

Several criteria are available in ABAQUS for crack growth analysis: critical stress, critical crack length versus time and critical crack opening displacement (COD). For ductile materials, critical COD is the most appropriate and it is used in this paper. This criterion is defined as:

$$g = \delta / \delta_c \,, \tag{4}$$

where δ is the current value of COD at some distance from the crack tip, while δ_c is the critical value of COD. Once the value g = 1.0 is reached, the condition is fulfilled and the node that is currently at the crack tip is being released.

Results and discussion

A comparison of the $CTOD_i$ values corresponding to crack initiation in SENB specimens is given in Fig. 3, determined both experimentally and using the GTN model. Very good agreement of the results is achieved for UM joints, and certain deviations appear for OM welds; the model gives higher values in comparison with the experimental ones. It seems that certain fraction of cleavage should be taken into account in case of OM joints. However, with GTN model it is possible to predict the effect of strength mismatching and to obtain lower values for the $CTOD_i$ in OM joints than in UM joints (see Fig. 3).

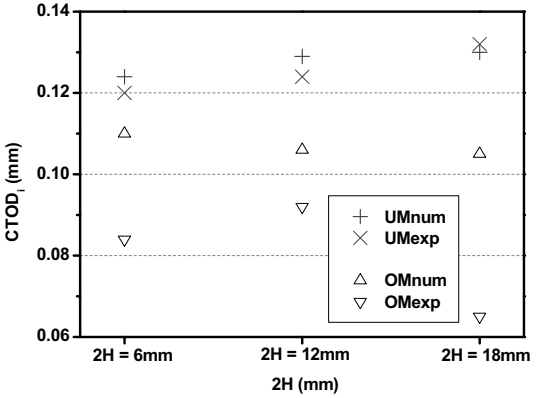

Fig. 3: Comparison of $CTOD_i$ obtained experimentally and using GTN model

As previously mentioned, $CTOD_i$ values in Fig. 3 are valid only for crack growth onset, i.e. releasing the first node. Conditions for releasing other nodes are different, due to the crack growth and subsequent change of geometry. Since $CTOD_i$ is determined indirectly in this paper, using critical void volume fraction f_c, criteria for releasing other nodes are not known in advance, but have to be calculated using an iterative procedure.

In the first iteration, it is assumed that the criteria for releasing of all nodes are the same, and initial deviations of f_c values in appropriate nodes are obtained. Based on these deviations, $CTOD_i$ values are defined for the next iteration, and the procedure is repeated until these deviations become so small that it can be said that the micromechanical criterion is fulfilled. This variation of $CTOD_i$ for overmatch joint 6mm wide is shown in Fig. 4, where *step* denotes the vertical displacement of

the cylinder for applying the load (Fig. 2) and *node* is the number of released nodes in front of the initial crack tip.

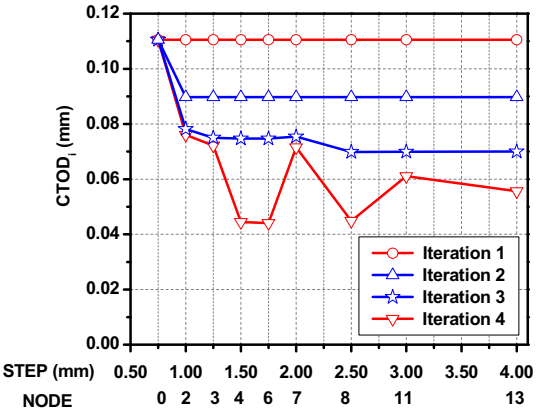

Fig. 4: Variation of CTOD$_i$ during the crack growth (OM 6 mm)

Fig. 5 shows graph F – CTOD for OM joint 6 mm wide with results of the first iteration (with the same CTOD$_i$ for all nodes), corrections including the effect of micromechanical criterion and experimental results. Corrected results include different value of CTOD$_i$ for each node, as explained in the previous paragraph, and it can be seen that the results are good, even without this correction, and both numerical results are similar to experimental ones. Results for other geometries and more details about the procedure can be found in [16]. It is shown that it is possible to use numerical results without the correction of CTOD$_i$ for each node. Concerning the comparison of numerical and experimental results, very good agreement is achieved for UM joints. For the crack growth in OM joints, numerical results are very good for 6 mm wide joints (as shown in Fig. 5), but they are less satisfactory for larger joint widths. The largest difference between experimental and numerical results is obtained for OM joints 18 mm wide. These deviations in case of OM joints might be the result of certain fraction of cleavage in fracture mechanism, same as for crack growth initiation.

The variation of J-integral, J_0, for OM and UM welded joints can be found in [8]. J_0 is computed using the procedure given in [18], and good agreement between experimental and numerical results is obtained, as shown in [8].

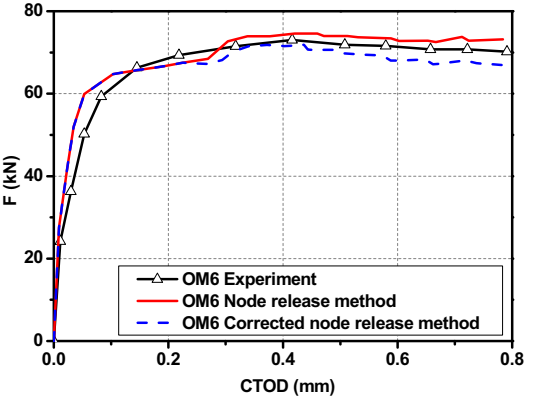

Fig. 5: F vs. CTOD for OM joints 6 mm wide

Summary

Experimental and numerical procedures have been used to analyse the constraint effect on over- and undermatched welded joints made of high-strength, low-alloyed steel. Crack initiation and growth of SENB specimen have been numerically simulated using the finite element method and micromechanical model of Gurson, Tvergaard and Needleman (GTN model). Metallographic observation has been used to quantify the volume fractions of non-metallic inclusions in materials. The highest volume fraction is found in base metal, while in UM and OM weld metals its values are smaller. Based on these data, initial void volume fraction, f_0, and mean free path between the inclusions, λ, have been determined.

In case of overmatching, higher constraint (i.e. larger joint width) causes more rapid increase of f in front of the crack tip, while the opposite trend has been observed in the analysis of the SENB specimen with undermatched weld metal. It is found that GTN model enables determination of the constraint effect caused by different widths of the weld metal on crack growth initiation. The model gives a good estimation of the crack growth onset for UM welded joints, while estimation of the crack growth onset for OM joints is not so good, probably due to certain amount of cleavage in addition to dominant ductile fracture mechanism. Further microstructural analysis of fractured specimens is needed to obtain the full insight into this phenomenon.

To get a complete understanding of the resistance of these joints to ductile fracture, stable crack growth has been analysed. During the simulation of stable crack growth, a combined technique has been developed – including the micromechanical approach and node release method. It has been shown that during the simulation of the crack growth, initial condition for the release of the first node can be used for the release of other nodes, despite the changed geometry due to the crack growth, still obtaining similar results. Comparison of numerical and experimental results revealed very good agreement in case of UM joints. For the crack growth in OM joints, numerical results are very good for 6 mm wide joints, but they are less satisfactory for larger joint widths. The explanation is the same as for crack growth initiation – deviations in case of OM joints might be the result of certain fraction of cleavage in fracture mechanism.

Obtained results can be used as a starting point for further investigations, extending to various crack locations in the welded joint. Further work should also include the application of micromechanical parameters determined on round tensile specimens and precracked specimens to welded structures and constructions. This would improve current methods for structural integrity assessment of the structures exposed to extreme working conditions.

Acknowledgements

The authors acknowledge the financial support of Serbian Ministry of Science under the project OI 144027 and Slo-Serb. bilateral project "Failure prevention of inhomogeneous materials and structures" (together with Slovenian Ministry of Science).

References

[1] K. H. Schwalbe: *Basic engineering methods of fracture mechanics and fatigue* (Geesthacht: GKSS-Forschungszentrum, Germany 2001)

[2] M. Kocak, editor: *Weld mis-match effect* (International Institute of Welding (IIW); France 1998)

[3] N. Gubeljak, I. Scheider, M. Kocak, M. Oblak, J. Predan, in: 14 European Conference on Fracture. EMAS Publ. (2002), p. 647

[4] *ESIS P6-98. Procedure to measure and calculate material parameters for the local approach to fracture using notched tensile specimens* (European Structural Integrity Society: ESIS, 1998)

[5] *ESIS P9-02D. Guidance on local approach of rupture of metallic materials* (European Structural Integrity Society: ESIS – Draft version, 2002)

[6] A. L. Gurson: Journ. Eng. Mater. Technol. Vol. 99 (1977), p. 2

[7] V. Tvergaard, A. Needleman: Acta Metallurg. Vol. 32 (1984), p. 157

[8] M. Rakin, N. Gubeljak, M. Dobrojevic, A. Sedmak: Engng. Fract. Mech. Vol. 75 (2008), p. 3499

[9] M. Dobrojevic, M. Rakin, N. Gubeljak, I. Cvijovic, N. Krunich, A. Sedmak: Mater. Sci. Forum Vol. 555 (2007), p. 571

[10] *ASTM. Standard practice for determining inclusion content of steel and other metals by automatic image analysis* (ASTM Standard E 1245-89, USA 1989)

[11] M. Rakin, A. Sedmak, V. Grabulov, N. Gubeljak, Z. Cvijovic, in: Proceedings of the 9th international conference on mechanical behaviour of materials, Geneva (2003)

[12] I. Penuelas, C. Betegon, J. J. del Coz: Engng. Fract. Mech. Vol. 73 (2006), p. 2756

[13] *GKSS:1991. Displacement gauge system for applications in fracture mechanics* (Patent Publication, Germany 1991)

[14] G. Bernauer, W. Brocks: *Numerical Round Robin on Micro-Mechanical Models – Results* (ESIS TC8, GKSS Research Center, Germany 2000)

[15] M. Rakin, Z. Cvijovic, V. Grabulov, S. Putic, A. Sedmak: Engng. Fract. Mech. Vol. 71 (2004), p. 813

[16] M. Dobrojevic: Crack growth modeling in welded joints, Ph.D Thesis, Faculty of Mechanical Engineering, Belgrade University (in Serbian) (2006)

[17] V. Las, J. Ocenasek, V. Vacek: Mater. Technol. Vol. 39(2005), p. 83

[18] ESIS P2-92. Procedure for determining the fracture behaviour of materials (European Structural Integrity Society: ESIS, 1992)